AD-A123 153 STRESSES DURING FABRICATION OF CYLINDRICALLY WOVEN CARBON-CARBON COMPOSIT..(U) CALIFORNIA UNIV LOS ANGELES SCHOOL OF ENGINEERING AND APPLIED.. G SINES ET AL. 1/1

UNCLASSIFIED 10 NOV 82 UCLA-ENG-82-78 N00014-77-C-0505 F/G 11/4 NL

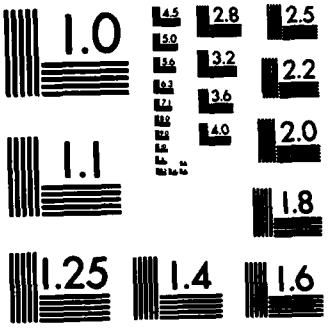

MICROCOPY RESOLUTION TEST CHART
NATIONAL BUREAU OF STANDARDS-1963-A

(12)

STRESSES DURING FABRICATION OF CYLINDRICALLY WOVEN CARBON-CARBON COMPOSITES

Interim Technical Report for period ending

October 31, 1982

Contract No. N00014-77-C-0505

Prepared for

Department of the Navy
Office of Naval Research
Arlington, Virigina 22217

George Sines and Jacob Cohen
Department of Materials Science and Engineering
School of Engineering and Applied Science
University of California
Los Angeles, California 90024

UCLA-ENG-82-78
November 1982

SECURITY CLASSIFICATION OF THIS PAGE *(When Data Entered)*

REPORT DOCUMENTATION PAGE

READ INSTRUCTIONS BEFORE COMPLETING FORM

1. REPORT NUMBER: UCLA-ENG-82-78	2. GOVT ACCESSION NO.: AD-A123153
3. RECIPIENT'S CATALOG NUMBER:	
4. TITLE *(and Subtitle)*: Stresses during Fabrication of Cylindrically Woven Carbon-Carbon Composites	5. TYPE OF REPORT & PERIOD COVERED: Interim Technical 8/1/81 - 10/31/82
	6. PERFORMING ORG. REPORT NUMBER: UCLA-ENG-82-78
7. AUTHOR(s): George Sines and Jacob Cohen	8. CONTRACT OR GRANT NUMBER(s): Contract N00014-77-C-0505
9. PERFORMING ORGANIZATION NAME AND ADDRESS: School of Engineering and Applied Science, University of California, (UCLA), Los Angeles, CA 90024	10. PROGRAM ELEMENT, PROJECT, TASK AREA & WORK UNIT NUMBERS:
11. CONTROLLING OFFICE NAME AND ADDRESS: Office of Naval Research, Arlington, Virginia 22217	12. REPORT DATE: November 10, 1982
	13. NUMBER OF PAGES: 13
14. MONITORING AGENCY NAME & ADDRESS *(if different from Controlling Office)*: Dr. L.H. Pebbles, ONR - Code 431, Arlington, Virginia 22217	15. SECURITY CLASS. *(of this report)*: unclassified
	15a. DECLASSIFICATION/DOWNGRADING SCHEDULE:

16. DISTRIBUTION STATEMENT *(of this Report)*

(none)

17. DISTRIBUTION STATEMENT *(of the abstract entered in Block 20, if different from Report)*

For public release

18. SUPPLEMENTARY NOTES

19. KEY WORDS *(Continue on reverse side if necessary and identify by block number)*

carbon
carbon-carbon composites
composites
cylindrical anisotropy
fabrication
fracture
rocket nozzle materials
thermal stress

20. ABSTRACT *(Continue on reverse side if necessary and identify by block number)*

Carbon-carbon billets sometimes experience failure during fabrication. In order to understand the stresses causing these failures, we have modeled the elastically anisotropic billet as an assembly of very thin-walled, isotropic cylinders. Alternate cylinders have different properties; one set models the fibers, the other the matrix. The assembly has cylindrical anisotropy and permits simple calculation of the thermal stresses of fabrication.

The stresses are calculated for the billet after cracks have been filled with pitch and reheated. A fabrication microcracking morphology is presented and

DD FORM 1 JAN 73 1473 EDITION OF 1 NOV 65 IS OBSOLETE
S/N 0102-LF-014-6601

SECURITY CLASSIFICATION OF THIS PAGE *(When Data Entered)*

ABSTRACT cont'd

the causes of this cracking discussed. The benefit of adding circumferential fibers to the inner and outer diameters is shown.

STRESSES DURING FABRICATION OF CYLINDRICALLY WOVEN CARBON-CARBON COMPOSITES

Interim Technical Report for period ending

October 31, 1982

Contract No. N00014-77-C-0505

Prepared for

Department of the Navy
Office of Naval Research
Arlington, Virigina 22217

George Sines and Jacob Cohen
Department of Materials Science and Engineering
School of Engineering and Applied Science
University of California
Los Angeles, California 90024

UCLA-ENG-82-78
November 1982

STRESSES DURING FABRICATION OF CYLINDRICALLY WOVEN CARBON-CARBON COMPOSITES

G. Sines and B. J. Cohen
University of California
Los Angeles, California

ABSTRACT

Carbon-carbon billets sometimes experience failure during fabrication. In order to understand the stresses causing these failures, we have modeled the elastically anisotropic billet as an assembly of very thin-walled, isotropic cylinders. Alternate cylinders have different properties; one set models the fibers, the other the matrix. The assembly has cylindrical anisotropy and permits simple calculation of the thermal stresses of fabrication.

The stresses are calculated for the billet after cracks have been filled with pitch and reheated. The benefit of adding circumferential fibers to the inner and outer diameters is shown.

NOMENCLATURE

Symbols

E	Young's Modulus, Psi
P	Pressure, Psi
R	Radius, in.
R	Radius after heating, in.
t	Thickness, in
T	Temperature, F
α	Thermal Expansion coefficient, /F

Subscripts

A	Axial direction in fiber bundle.
C	Circumferential direction in billet.
F	Fiber
i	inside
M	Matrix
n	cylinder's number
o	outside
R,rr	Radial direction in billet.

T Transverse
Z Axial direction in billet
(n,n+1) Inter-cylinder

Superscripts

E Elastic Effect
T Thermal Effect

INTRODUCTION

Carbon-carbon composites may have some structural anomalies which can hinder their use in rocket nozzles. These probably can be reduced by understanding the stresses occurring during processing and then making appropriate processing changes. The purpose of this study was to develop a model to predict the stresses which occur during processing of cylindrically woven carbon-carbon composites. There does exist very sophisticated complex programs for calculating stresses in shapes having cylindrical symmetry made of materials having cylindrical anisotropy. These programs, called DCAP and SAAS I, II, III, have complexities that discourage their use for the much simpler problem considered here and for which approximate solutions can be useful.

The densification process of the billet consists of repeated impregnation, carbonization, and graphitization using pitch as the impregnant. Upon heating to the first graphitization temperature of 5000°F (2750°C), because of the differences in coefficient of thermal expansion for the fibers and the matrix, the matrix expansion and fiber anisotropy induces tensile stresses within the fibers and compressive ones in the interstitial matrix pockets. The transverse expansion of the fibers and also the expansion of the matrix pockets tends to close the cracks generated during the previous carbonization cycle. Both the radial and circumferential composite expansion are higher than the axial expansion of the circumferential fiber bundles, resulting in highly stressed circumferential bundles.

Since the billet is kept at the higher graphitization temperature for a matter of hours, it is thought that it becomes stress-free at that temperature due to creep. Upon cooling from this peak temperature, cracks occur in the matrix from thermal stresses induced by the anisotropic contractions of fiber bundles and the constraint of circumferential fiber bundles which have a higher elastic modulus and lower coefficient of thermal expansion in their axial direction than the matrix. The matrix is stressed in tension since it tries to contract at a much higher rate than the fiber bundles. This results in cracks occurring between the fiber bundles and the matrix pockets [1,2].

The cycle is repeated in order to fill up those voids which are connected by the cracks generated during the cooling from the previous graphitization step. The degree of penetration depends upon the processing conditions such as crack size, crack size distribution, and gas permeability.

PROCESSING STRESSES

During the fabrication of cylindrically woven carbon-carbon composites, fractures and/or waviness sometimes occur in the circumferential bundles. The large scale fractures and waviness which may be catastrophic are caused by the cylindrical anisotropy of the thermal expansion and of the elastic moduli.

If the billet was reheated to the previous graphitization temperature before reimpregnation, the cracks would just close and the billet would be stress-free as it had been at the end of the previous graphitization step. However, if the cracks are filled with pitch, which is the case in the next reimpregnation step, very high stresses would occur in the fiber bundles during reheating to the graphitization temperature. The high transverse thermal expansion of the circumferential fibers as well as that of the matrix will cause a high tensile stress in the circumferential fibers at the outer radii and a high compressive one at the inner radii of the billet.

Stress Calculations

In this study the billet is modeled as an assembly of concentric thin-walled cylinders. Alternate cylinders have different properties: one set models the fiber, the other the matrix. the number of cylinders modeling the fibers are equal to the number of layers of circumferential wraps. The billet used in this study had 60 cylinders (numbered from one to 60). The odd numbers are for the fiber cylinders and the even numbers the matrix ones.

The anisotropy stresses can be found by giving each set of cylinders elastic moduli and thermal expansion coefficients which represent the fiber's properties and the other the matrix properties. The stresses are obtained by assuming that the properties of the fiber and the matrix cylinders will not change with temperature and also the cylinders are initially in stress-free contact. A change in temperature causes the cylindrical diameters to change and thereby introduces inter-cylindrical pressures throughout the billet radii.

Inter-cylindrical Pressures - To find the approximate mean value for the hoop, $\sigma_{\theta\theta}$, and radial stresses, σ_{rr}, along the radius of the billet, one needs to calculate the pressure at each inter-cylinder surface and use the following equation

$$\sigma_{\theta\theta} = \frac{\Delta P_n R_n}{t_n} = \frac{(P_i - P_o)_n R_n}{t_n} - P_o \qquad (1\text{-a})$$

$$\sigma_{rr_n} = \frac{(P_i + P_o)_n}{2} \qquad (1\text{-b})$$

where R is the mean radius, t the thickness, P_i the internal pressure, P_o the external pressure, R_o the outer radius, R_i the inner radius, and n refers to the n^{th} cylinder.

In the following calculations the second term of Eq. (1-a), $-P_o$, was omitted. It has influence at the mid-radius but at the outer and inner radii its direct effect is negligible. It might have some effect on the calculation of the circumferential stress distribution. Also Poisson's ratio has been taken to be zero.

As temperature increases, two radial changes must be considered:

1) free thermal changes of the mean radius,

$$\Delta R_n^T = R_n \alpha_n \Delta T \qquad (2)$$

2) elastic change of the mean radius,

$$\Delta R_n^E = \frac{\Delta P_n R_n^2}{t_n E_n} \tag{3}$$

where α_n is the coefficient of thermal expansion, ΔP is the pressure difference, and the t_n is the thickness of the n^{th} cylinder.

$$\Delta R^{Total} = \Delta R_n^T + \Delta R_n^E \tag{4}$$

The relation between the radii of the two neighboring inter-cylinders before and after the temperature change with no elastic constraint are

$$R_{(n+1,n+2)} = R_{(n,n+1)} + t_{n+1} \quad \text{before} \tag{5}$$

$$R'_{(n+1,n+2)} = R'_{(n,n+1)} + t_{(n+1)}\ (1+\alpha_{(n+1)}\Delta T) \quad \text{after} \tag{6}$$

where $R_{(n+1,n+2)}$ is the outer radius of the $(n+1)^{th}$ cylinder, $R_{(n,n+1)}$ is the inner radius of the $(n+1)^{th}$ cylinder and $t_{(n+1)}$ its thickness and R' the radius after temperature change.

The radius of the inner surface of the $(n+1)^{th}$ cylinder with the thermal and elastic strains is

$$R'_{(n,n+1)} = R_{(n,n+1)} + \Delta R_{total(n)} \tag{7}$$

$$R'_{(n,n+1)} = R_{(n,n+1)} + \frac{\Delta P_n R_n^2}{t_n E_n} + R_{(n,n+1)}\alpha_{(n+1)}\Delta T \tag{8}$$

The billet used for this calculation has four different circumferential zones. In the first and second zone the fiber cylinders thicknesses are the same. In the third zone the fiber cylinders have twice the thickness of the first two, and the fourth zone they are twice that of the third. The matrix cylinders have constant thicknesses in all four zones. There is only one fiber type used for the circumferential wrapping; therefore, the thermal expansion coefficient and moduli of elasticity are constant along the radius of the billet. The coefficient of thermal expansion is for the longitudinal direction of the fiber. The transverse thermal expansion of the fiber cylinder is added to that of the matrix cylinder by using the sum of the transverse coefficient of expansion of the fiber and the coefficient of the matrix material. This introduces an approximation because the thickness of the matrix cylinders at the inner radius of the billet are more[1] than that of the fiber at the inner and less at the outer radius.

1 The analysis is simplified by having the materials for both, matrix and fiber cylinders, isotropic. It is important to insert the high transverse thermal expansion of the fibers,and it is done by combining it with that of the matrix.

For each cylinder, substituting the R generated from equation (8) into equation (6) one can write

$$R_{(n,n+1)} + \frac{\Delta P_{(n+1)} R^2_{(n+1)}}{t_{(n+1)} E_{(n+1)}} + R_{(n,n+1)} \alpha_{(n+1)} T + t_{(n+1)} (1+\alpha_{(n+1)} \Delta T) =$$

$$R_{(n+1,n+2)} + \frac{\Delta P_{(n+2)} R^2_{(n+2)}}{t_{(n+2)} E_{(n+2)}} + R_{(n+1,n+2)} \alpha_{(n+2)} \Delta T \qquad (9)$$

$\alpha_{(n+1)} = \alpha_F$ when n is even and $\alpha_{(n+1)} = \alpha_M$ when n is odd, and similarly for E and where $R_{(n,n+1)} + t_{(n+1)} = R_{(n+1,n+2)}$

Solving equation (9) for each cylinder gives

$$\frac{\Delta P_{(n+2)} R^2_{(n+2)}}{t_{(n+2)} E_{(n+2)}} - \frac{\Delta P_{(n+1)} R^2_{(n+1)}}{t_{(n+1)} E_{(n+1)}} = R_{(n+1,n+2)} (\alpha_F - \alpha_M) \Delta T \qquad (10)$$

where $\Delta P_{(n+2)} \equiv P_{(n+1,n+2)} - P_{(n+2,n+3)}$ and

$$\Delta P_{(n+1)} \equiv P_{(n,n+1)} - P_{(n+1,n+2)}$$

By substituting the value of the mean radius, intercylindrical radius, the thickness of each cylinder, the value of moduli of elasticity, coefficients of thermal expansion and choosing a temperature change, a set of 59 algebraic equations are generated in which only the pressure at the inter-cylinders are unknown. There are 59 unknown pressures in these 59 equations, where three of the unknowns are in each equation except the first and last which contain only two unknowns because the internal and external pressures of the billet are zero.

These 59 equations were solved by using a subroutine program, LEQT2F, in IBM 3033 computer. The value of those inter-cylindrical pressures are given in Fig. 1. These pressures can be used to calculate the hoop fiber and radial fiber stresses which are caused by cylindrical anisotropy. The radial stresses of the billet, shown in Fig. 1, are almost equal to the negative of the inter-cylindrical pressures for each cylinder, they being the negative of the average of the inter-cylindrical pressures on the two sides of a cylindrical element.

The inter-cylindrical pressure can now be inserted into equation (1a) to obtain the hoop stresses in the fiber cylinders which are given in Fig. 2. The accuracy of the inter-cylindrical pressures as read from Fig. 1 would not have sufficient accuracy to make these calculations which involve small differences of large numbers. These pressures were in double precision in the computer calculations. The above calculation of the fiber stress depended on measured constituent properties. It can be confirmed by direct measurement of the crack opening which occurs upon cooling from the graphitization. Assuming that the matrix has little tensile strength and that the radial fibers are debonded, the radial strain should be equal to the sum of crack openings divided by the radial distance. When these cracks are filled by re-impregnation and the billet is reheated to the graphitization temperature this material stuffed in the cracks must be accommodated by elastic strain.

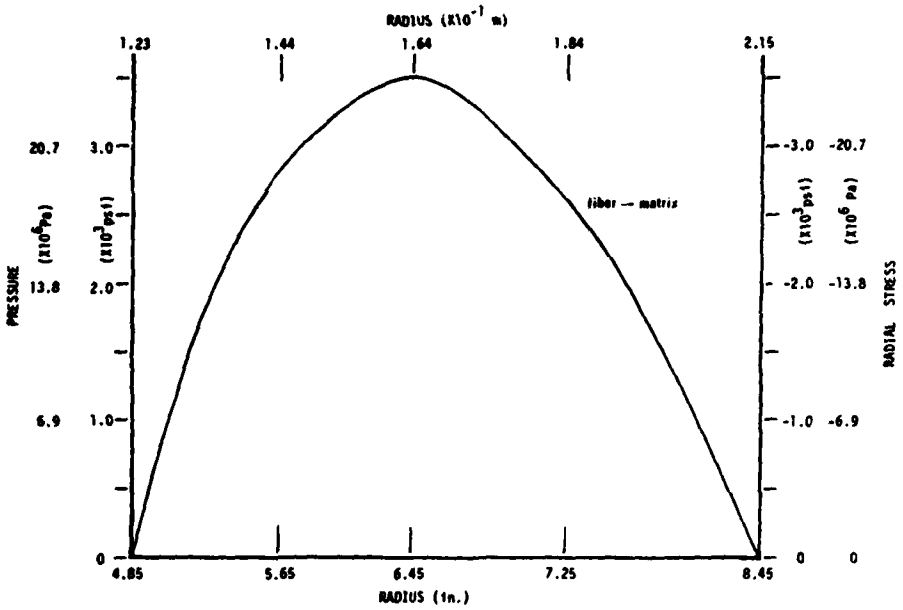

Fig. 1. Calculated intercylinder pressures and radial stresses.

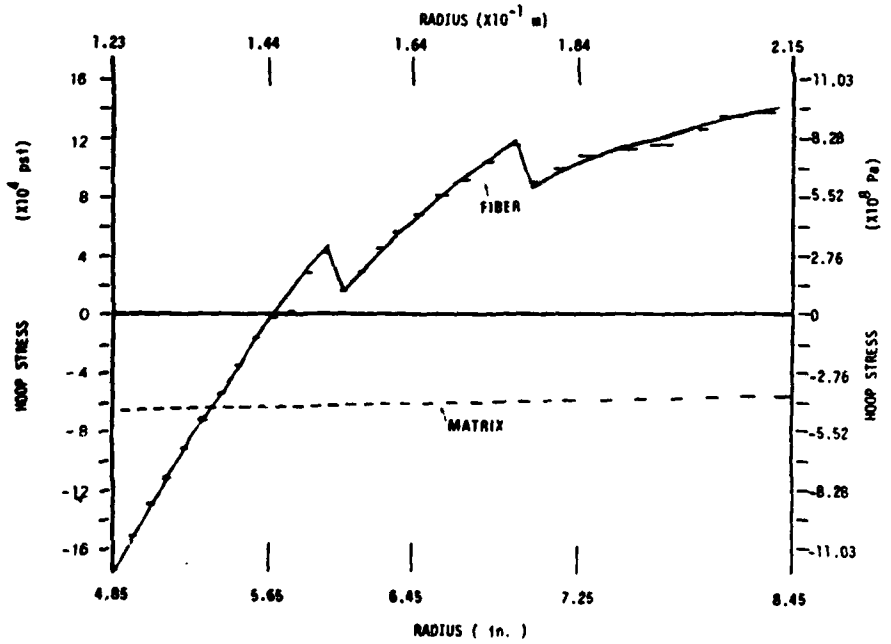

Fig. 2. Calculated hoop stresses.

CRACK MORPHOLOGY

The morphology was determined by examining the crack traces on planes making equal angles with the r, θ, and Z-directions, Fig. 3. The quantitative, statistical analysis of the circumferential crack openings on θ-Z plane, in the radial direction were made on transverse slices of the r-θ plane (Fig.20 of Reference 1.). The average presented in Fig. 4 are for 24 traverses (every 15 degrees) on the billet. The matrix fractures were different in the three regions of measurement. In the central section the normalized crack opening (strain relieved by cracking) was 3.81×10^{-3} the average over the three sections being 3.64×10^{-3}. (The billet had four regions but the innermost region had been machined off before we received it.)

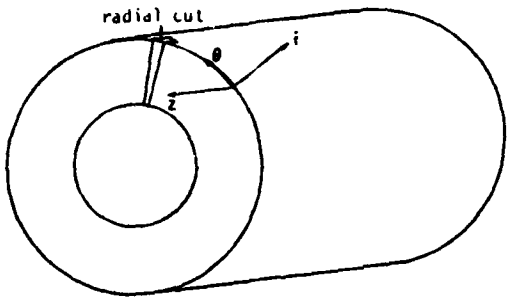

Fig. 3a. Cylindrical billet and a radial cut.

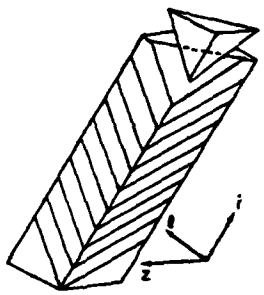

Fig. 3b. Nine slices of (111) plane on radial sample.

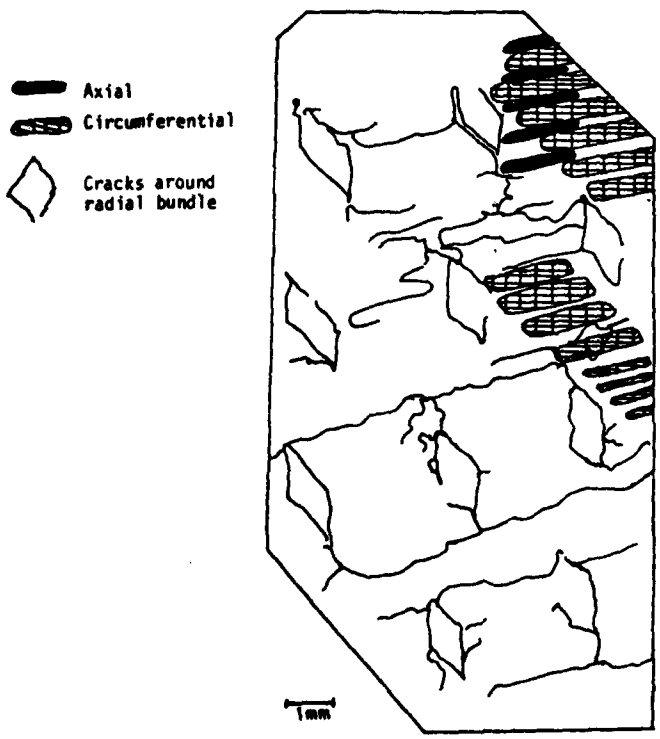

Fig. 3c. Traces of circumferential cracks (θ-z) on (111) plane

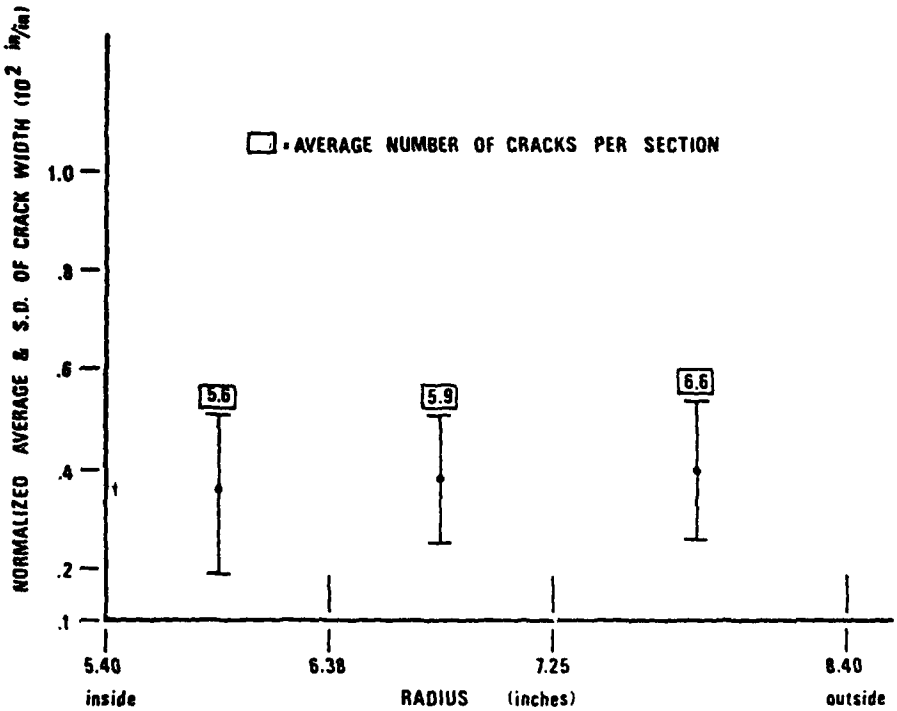

Fig. 4. Crack openings in the radial direction for crack planes on the (θ - r) plane.

We have made a detailed study of the fabrication cracks in two billets. This revealed the following results: (1) An extensive crack structure is seen in the circumferential plane (Z-θ plane) which tends to be periodic; cracks tend to occur after each five or six circumferential fibers, (2) Each radial fiber is surrounded by cracks or at least on three sides. These cracks are continuous along the radial fibers through the billet, (3) There are a few cracks around some axial fibers, (4) Toward the outer radii the circumferential cracks are short and scattered so that the tracing of them is not possible, (5) About 60% of the observed crack length is circumferential and about 40% surrounds the radial fibers.

Semi-quantitative prediction of the amount of crack opening may reveal what is happening during fabrication. First let us assume that at the graphitization temperature (a) creep and property changes result in a stress-free state, (b) upon cooling the radial fibers debond and remain stress-free, (c) transverse tensile strength of the fibers and that of the matrix is negligible.

The change in radial distance between the outermost circumferential bundles at radius R_o and the innermost at R_i upon cooling ΔT is

$$-(R_o - R_i)\,\alpha_A\,\Delta T \qquad (11)$$

where α_A is the coefficient of thermal expansion along the axis of the bundle. The change in radial distance considering the transverse contraction of the fibers and of the matrix upon cooling is

$$-(R_o - R_i)\,\alpha\Delta T \qquad (12)$$

where α is an appropriately weighted average of the coefficient of thermal expansion of the fibers in the transverse direction and that of the matrix. The amount of normalized crack opening then would be

$$\frac{(R_o - R_i)\alpha\,\Delta T - (R_o - R_i)\alpha_A\,\Delta T}{(R_o - R_i)} = (\alpha - \alpha_A)\,\Delta T \qquad (13)$$

Using $\alpha_A = 1.4 \times 10^{-6}\ F^{-1}$, $\alpha = 6.6 \times 10^{-6} F^{-1}$, and $\Delta T = 5000^{\circ}F$, where the alphas are approximate median values based on many reports and are probably valid to one significant figure, the calculated normalized crack opening is 26×10^{-3}.

Figure 4 shows values of crack openings which are typical of those of one billet measured in Reference 1. Notice that the average measured value is about 3.6×10^{-3}. This value is an order of magnitude less than that predicted. This discrepancy may indicate that the stress has not been completely relieved at the graphitization temperature. It must be remembered that no creep data has been published for graphitized impregnated bundles; estimates of stress relief have been made from creep studies on bulk graphite.

On the other hand, one could make the assumption that stress still exists at the graphitization temperature. Therefore, superimposed on the above must be the elastic changes of the billet that occur upon cooling from graphitization. Because of the tensile stresses at the outer radii of the billet, the elastic strain tends to reduce its radius whereas at the inner radius, since the stresses are compressive, the radius increases. These changes in radii tend to close some of the cracks mentioned above. Furthermore the matrix material between the outermost and innermost radius being in compression will expand upon release of the thermal stress. This elastic closure should account for much of the difference between the predicted value of crack opening and that observed.

The stress at the start of cooling from graphitization must be very dependent on the thermal history within the billet which may not be known exactly. The second billet studied in Reference 1 had about three times the normalized crack opening of the one cited above which would be consistent with much more stress relief.

The above is only an order of magnitude calculation. It does reveal the following:

1. to reduce cracking a pitch should be selected so that at graphitization temperature it has a minimum reduction in volume,

2. the graphitization temperature should be as low as possible to minimize relief of stress due to creep in the circumferential bundles.

The above calculation is an elastic one assuming a continuous medium, that is, the cracks have been, filled and therefore reversible behavior should occur upon cooling form the graphitization temperature, the billet should return to the assumed initial stress-free state. It has not accounted for the decrease in volume which occurs during carbonization and graphitization of the pitch which was added in the last impregnation. If this is considered, it is not a reversible process but residual stresses would exist at the lower temperature which would have signs opposite to those at the higher temperature and of an amount equal to (change in density of the pitch/initial density of the pitch) of those at the higher temperature. This does substantially reduce the calculated stresses. These residual stresses are fictitious ones introduced by the model. In the billet these stresses should be greatly relieved by extensive cracking.

WRAPPING

Overwrapping

To calculate the processing stress levels of the billet, it was assumed that five fiber wraps of the same type and size as the outer radii fiber bundles were added to the outer diameter of the billet during preform fabrication. Calculated stress levels of this billet showed a shift of high tensile stresses the outer diameter to the overwrap region thereby causing a reduction in the stress levels of the main billet's outermost fiber.

Underwrapping

The addition of five fiber wraps of the same type and size to the inner diameter of the billet was assumed during fabrication of the preform. The calculations showed a reduction on the compressive stress levels at the innermost hoop fiber of the main billet slightly more than at the outermost. This can reduce the possibility of buckling of the inner radii hoop fibers.

Overwrapping is a process that needs little clarification but "underwrapping" does. One way to achieve this is to have a cylindrical mandrel of bulk graphite around which is wrapped the extra circumferential bundles of the underwrapping. The bundles of billet are then laid-up on this mandrel and the assembly impregnated, carbonized and graphitized. The extra support provided by the circumferential bundles at the inner bore would reduce compression on the bore occurring on cooling from graphitization.

Over- and Underwrapping - Assuming the addition of over and underwraps to the billet will have the combined effects both of which introduces a lower processing stress levels into the entire billet. Fig. 5 shows their combined effect. This model does not calculate the full amount of the stress in the wrapping because it does not include the intersurface pressures from the transverse thermal expansion of the added bundles. Even so, the possibility of rupture should be reduced because all of the fibers in these added cylinders are in the circumferential direction, the bundles are free of stress variations caused by adjacent bundles transverse to them, and the bundles are free from the stress caused by the expansion of matrix pockets.

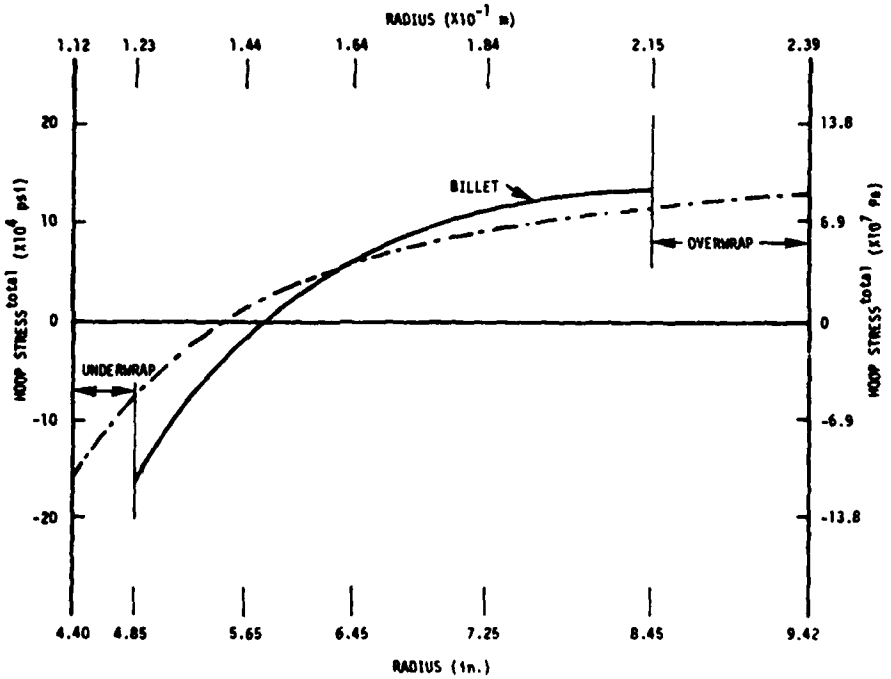

Fig. 5. Effect of underwrap and overwrap on hoop fiber stresses.

DISCUSSION

It must be emphasized that the stresses predicted in this report are impossible to measure and the validity of the many assumptions that were made cannot be checked; however, the damage caused by them is real and observable. The calculations based on our model show general trends which agree with calculations based on quite different models. The anisotropic thermal stress distribution based on a continuum model and calculated by the SAAS Program, [Reference 3, Fig. B6] and that presented from calculations on our heterogeneous model in Fig. 1 have the same general features as our concentric cylinder model. This agreement gives confidence in both of the models, even though use of different material properties and lay-up prevents quantitative comparison. (The magnitude of the stresses in Fig. B5 of Reference 3 are for the synthetic composite continuum, whereas the ones in Fig. 1 are just for the fibers and therefore they are not directly comparable.)

We are aware that the properties change with temperature, with repeated thermal treatments, and that carbon is not linearly elastic. We also acknowledge that the properties assigned to the two types of cylinders are a synthesis: the "fiber" cylinders contains some matrix and the "matrix" cylinders account for the transverse properties of the fiber bundles. The values used for their properties might be refined by more careful consideration of the interaction of their constituents in the manner used in Reference 4.

CONCLUSIONS

(a) It has been shown here that the stresses which occur by filling the cracks with pitch and then reheating to the graphitization temperature are appreciable. These stresses have a tensile maximum in the circumferential fibers at the outer radius of the billet and a compressive one at the inner radius. These stresses have probably caused the failures which have occurred during fabrication.

(b) The analysis has shown that overwrapping can transfer the peak tensile stuffing stress from the billet to the overwrapping and thereby might prevent billet failure. The overwrap would have higher strength than the outer layers of the billet because the overwrap can have all the fiber bundles oriented in the direction of the peak stress.

(c) The analysis also shows that "underwrapping", that is adding material at the inner radius, can transfer the maximum compressive stuffing stresses away from the billet. It should be possible to design an underwrap with a higher compressive strength than the billet.

(d) Using pitch with low reduction in volume on carbonization and densification should minimize cracking.

(e) Graphitization at the lowest feasible temperature should also minimize cracking.

(f) It has been observed that the cracking which occurs upon cooling from graphitization consists primarily of circumferential cracks. This morphology should be considered in service stress calculations and in consideration of ablation.

(g) It has been observed that most of the radial bundles are enclosed by a continuous crack extending from the bore to the outside of the billet. The function of the radial bundles during fabrication and use should be re-evaluated.

(h) Comparison of measured crack openings with order-of-magnitude calculations indicate that during graphitization the billet may not have all of the stress relieved.

ACKNOWLEDGEMENT

Professor S.B. Batdorf of UCLA, and Steve Evangelides of Science Applications contributed to many aspects of the project. This work was sponsored by ONR; Dr. L.H. Peebles is the technical monitor. The authors would like to thank Julius Jortner for the several stimulating and provocative discussions.

REFERENCES

1. George Sines, et al, "Damage Mechanisms and Modeling of Carbon-Carbon Composites", UCLA-ENG-81-26, Sept. 1981, University of California, Los Angeles.

2. Julius Jortner, "Cracking in 3-D Carbon-Carbon Composites and Effects on Performance", Proceedings of the Army Symposium on Solid Mechanics, AMMRC - MS, Sept. 76, pp. 81-97.

3. J. Kibler, K. Buesking, "Nosetip and Rocket Nozzle Carbon/Carbon Material Evaluation" Final Report N60921-77-C-0230, June 1978, Materials Sciences Corporation, Blue Bell, PA.

4. K. Buesking, et al. "Nozzle Material Design Study" Final Report N60921-78-C-0218, Sept. 1979, Materials Sciences Corporation, Blue Bell, PA.

DISTRIBUTION LIST

CARBON MATERIALS PROGRAM

Restricted Export Control Laws Distribution (unknown University people deleted)

Acurex/Aerotherm
Attn: Mr. H. Tong
485 Clyde Avenue
Mountain View, CA 94042

Acurex/Aerotherm
Attn: Dr. J. E. Zimmer
435 Clyde Avenue
Mountain View, CA 94042

Acurex/Aerotherm
Attn: Mr. D. L. Carlson
485 Clyde Avenue
Mountain View, CA 94042

Dr. D. F. Adams
Department of Mechanical Engineering
University of Wyoming
Laramie, WY 82071

Mr. D. Walrath
Department of Mechanical Engineering
University of Wyoming
Laramie, WY 82071

Aerojet
Attn: Mr. J. Cauzza
PO Box 13400
Sacramento, CA 95813

Aeronutronic-Ford
Attn: Mr. J. Perry
Ford Road
Newport Beach, CA 92663

Aerospace Corporation
Attn: Mr. R. A. Meyer
PO Box 92957
Los Angeles, CA 90009

Aerospace Corporation
Attn: Mr. J. L. White
PO Box 92957
Los Angeles, CA 90009

Aerospace Corporation
Attn: Mr. G. S. Rellick
PO Box 92957
Los Angeles, CA 90009

Aerospace Corporation
Attn: Dr. L. Rubin
PO Box 92957
Los Angeles, CA 90009

Air Force Materials Laboratory
AFML/MB (Mr. J. Kelble)
Wright-Patterson AFB, OH 45433

AF Office of Scientific Research
Building 410
Bolling AFB, DC 20332

AF Rocket Propulsion Laboratory
AFRPL/MK (Dr. C. Hawk)
Edwards AFB, CA 93523

AF Rocket Propulsion Laboratory
AFRPL/MKBN (L. Tepe)
Edwards AFB, CA 93523

AF Weapons Laboratory
Attn: L/C D. Ericson
Kirtland AFB, NM 87117

AFML/MBC (Mr. D. Schmidt)
WPAFB, OH 45433

AFML/MX (Dr. M. Minges)
WPAFB, OH 45433

AFML/MXE (Mr. J. Latva)
WPAFB, OH 45433

AFRPL/MKCC (Mr. W. Payne)
Edwards AFB, CA 93523

Army Materials & Mechanics Research
Attn: AMXMR (H. J. Dignam)
Watertown, MA 02172

Atlantic Research Corporation
Attn: Mr. J. Bird
5290 Cherokee Avenue
Alexandria, VA 22314

Atlantic Research Corporation
Attn: Mr. R.S. Frankle
5390 Cherokee Avenue
Alexandria, VA 22314

AVCO Corporation
Attn: Mr. Dale Dallan
Lowell Industrial Park
Lowell, MA 01851

AVCO Corporation
Attn: Mr. T. Laskaris
Lowell Industrial Park
Lowell, MA 01851

AVCO Corporation
Attn: Mr. P. Rolincik
201 Lowell Street
Wilmington, MA 01887

Dr. R. L. Baker
Aerospace Corporation
PO Box 92957
Los Angeles, CA 90009

Dr. S. Batdorf
School of Engineering & Applied Science
University of California, Los Angeles
Los Angeles, CA 90024

Battelle Memorial Institute
Attn: Mr. W. Chard
505 King Avenue
Columbus, OH 43201

NASA
Attn: Mr. Charles F. Bersch, RTM-6
Washington, DC 20546

California Research and Technology, Inc.
Attn: Dr. K. Kreyenhagen
6269 Daniel Avenue
Woodland Hills, CA 91364

Corborundum Company
Graphite Products Division
Attn: Mr. W. Carlson
2050 Cory Drive
Sanborn, NY 14132

Dr. R. J. Diefendorf
Dept. of Materials Engineering
Rensselaer Polytechnic Institute
Troy, NY 12181

Director
Defense Nuclear Agency
Attn: Mr. D. Kohler
Washington, DC 20305

Mr. R. J. Edwards
Code R31
NSWC/WOL
Silver Spring, MD 20910

Effects Technology, Inc.
Attn: Mr. M. Graham
5383 Hollister Avenue
Santa Barbara, CA 93105

Effects Technology, Inc.
Attn: Mr. W. Fadler
5383 Hollister Avenue
Santa Barbara, CA 93105

Mr. D. Ehrentreis
Consulting Engineer
5 Horizon Road
Fort Lee, NJ 07024

Mr. J. S. Evangelides
Science Applications, Inc.
18872 Bardeen
Irvine, CA 92715

Fiber Materials, Inc.
Attn: Mr. L. McAllister
Biddeford Industrial Park
Biddeford, ME 04005

Dr. J. Gebbhardt
General Electric Company
RESD, Room 2023
PO Box 7560
Philadelphia, PA 19406

General Electric Company
RESD, Room 2023
Attn: Dr. E. Stover
PO Box 7560
Philadelphia, PA 19406

General Electric Company
RESD, Room 2023
Attn: P. Bolinger
PO Box 7560
Philadelphia, PA 19406

Great Lakes Carbon Corporation
Attn: Mr. W. Benn
299 Park Avenue
New York, NY 10017

irector
trategic Systems Project Office (PM-1)
tn: Dr. J. Kincaid (Code SP-20)
epartment of the Navy
shington, DC 20376

irector
trategic Systems Project Office (PM-1)
tn: Mr. S. Weinger (Code SP)
epartment of the Navy
shington, DC 20360

per-Temp Company
tn: Mr. D. Bauer
11205 Norwalk Boulevard
anta Fe Springs, CA 90670

ystems, Science and Software
tn: Dr. G. Gurtman
O Box 1620
a Jolla, CA 92037

hiokol
tn: Mr. G. Broman
righam City, UT 84302

roject Manager
rident Systems Project (CNM-PM 2)
tn: Mr. J. Crone (Code HM-2-001)
epartment of the Navy
ashington, DC 20360

RW Systems Defense Space Systems
tn: Dr. W. Kotlensky
ldg. R-1-Room 2012
ne Space Park
edondo Beach, CA 90278

RW Systems Defense Space Systems
tn: R. Szymanski
ldg. R-1-Room 2012
ne Space Park
edondo Beach, CA 90278

r. D. R. Uhlmann
ept. of Materials Sciences & Engineering
lass. Institute of Technology
ambridge, MA 02139

r. D. R. Ulrich
ldg. 410
FOSR/NC
olling AFB, DC 20332

Union Carbide Corporation
Nuclear Division (Y-12 Plant)
Attn: Mr. A. Taylor
PO Box Y
Oak Ridge, TN 37839

Union Carbide Corporation
Carbon Products Division
Attn: Mr. J. Bowman
PO Box 6116
Cleveland, OH 44101

United Technologies
Chemical Systems Division
Attn: Mr. R. Ellis
PO Box 358
Sunnyvale, CA 94088

U.S. Energy Research Division Administratio
Attn: Mr. A. Littman
Nuclear Research & Application Division
Washington, DC 20331

Department of Mining, Metallurgical
and Ceramic Engineering
Attn: Dr. D. Fischbach
University of Washington
Seattle, WA 98195

Mr. R. Wilson
Code R31
NSWC/WOL
Silver Spring, MD 20910

Office of Naval Research, Code 431
800 North Quincy Street
Arlington, VA 22217 2 copies

Defense Technical Information Center
Building 5 Cameron Station
Alexandria, VA 22314 12 copies

Office of Naval Research
Attn: Code 413
800 North Quincy Street
Arlington, VA 22217

Office of Naval Research
Eastern/Central Regional Office
Attn: Dr. L. H. Peebles, Jr.
666 Summer Street
Boston, MA 02210 2 copies

Office of Naval Research, Code 430
Attn: Dr. A. M. Diness
800 North Quincy Street
Arlington, VA 22217

NETCO
Attn: Mr. W. Pfeifer
110 Pine Avenue, Suite 906
Long Beach, CA 90802

Dr. G. G. Ormbrek (2 copies)
AFWAL/MLSE
WPAFB, OH 45433

OSD/DDR&E
OAT/ET (Mr. J. Persh)
Washington, DC 20301

Dr. N. Pagano
AFWAL/MLBM
WPAFB, OH 45433

Department of Defense
Plastics Technical Evaluation Center
Attn: Mr. A. Anazione, Bldg. 176
Picatinny Arsenal
Dover, NJ 07801

Dr. Robert Pohanka (Code 431)
Office of Naval Research
Department of the Navy
Arlington, VA 22217

Prototype Development Associates, Inc.
Attn: Dr. G. Crose
1740 Garry Avenue, Suite 201
Santa Ana, CA 92705

Prototype Development Associates, Inc.
Attn: Mr. E. L. Stanton
1740 Garry Avenue, Suite 201
Santa Ana, CA 92705

C. R. Rowe
Code R31
NSWC/WOL
Silver Spring, MD 20910

Dr. Fred E. Saalfeld
Code 6100
Naval Research Laboratory
Washington, DC 20375

SAMSO/ABRES (L/C J. McCormack)
Worldway Postal Center
PO Box 92960
Los Angeles, CA 90009

SAMSO/MNPX (Capt D. Bailey)
Norton AFB, CA 92409

Sandia Laboratories
Attn: Mr. D. Northrup
PO Box 5800
Albuquerque, NM 87185

Sandia Laboratories
Attn: D. J. Rigali
PO Box 5650
Albuquerque, NM 87185

Science Applications, Inc.
Attn: Mr. D. Eitman
201 W. Dyer Road, Unit C
Santa Ana, CA 92707

Science Applications, Inc.
Attn: Mr. K. Kratsch
201 W. Dyer Road, Unit C
Santa Ana, CA 92707

Science Applications, Inc.
Attn: Mr. W. C. Loomis
201 W. Dyer Road, Unit C
Santa Ana, CA 92707

Dr. G. Sines
School of Engineering & Applied Scienc
University of California, Los Angeles
Los Angeles, CA 90024

Southwest Research Institute
Attn: Mr. Craig Robinson
San Antonio CA 78200

Southern Research Institute
Attn: Mr. H. Starrett
2000 Ninth Avenue, South
Birmingham, AL 35205

Southern Research Institute
Attn: Mr. C. Pears
2000 Ninth Avenue, South
Birmingham, AL 35205

Southwest Research Institute
Attn: Dr. J. Lankford
P.O. Drawer 28510
San Antonio, TX 78284

Space and Missile Systems
SAMSO/MNNR (Capt T. Brocato)
Norton AFB, CA 92409

Stackpole Fibers Company, Inc.
Attn: Mr. G. Fleming
Foundry Industrial Park
Lowell, MA 01852

Great Lakes Research Corporation
Attn: Mr. H. Gilliam
PO Box 1031
Elizabethton, IN 37643

HAVEG
Attn: Mr. R. Pegg
12827 East Imperial Highway
Santa Fe Springs, CA 90670

Hercules Corporation
Attn: Mr. P. Christensen
PO Box 93
Magna, UT 84044

HITCO
Attn: Mr. L. Dyson
1600 West 135th Street
Gardena, CA 90249

Dr. R. J. Houston, MS 231
NASA
Langley Research Center
Hampton, VA 23665

Mr. Edward Jeter, Code 3242
Naval Weapons Center
China Lake, CA 93555

Jet Propulsion Laboratory
Attn: Mr. N. Kimmel
Pasadena, CA 91103

Mr. Julius Jortner
Science Applications, Inc.
18872 Bardeen
Irvine, CA 92715

Kaiser
Attn: Mr. M. Fischer
880 Doolittle Drive
San Leandro, CA 94577

Mr. F. J. Koubeck
Code R31
NSWC/WOL
Silver Springs, MD 20910

Lawrence Livermore Laboratories
Attn: Mr. A. Maimoni (L-503)
PO Box 808
Livermore, CA 94550

Lockheed Missiles and Space Company
Attn: Dr. M. Steinberg
PO Box 504
Sunnyvale, CA 94088

Los Alamos Scientific Laboratory
Attn: Dr. J. Taylor
University of California
PO Box 1663
Los Alamos, NM 87545

Dr. Carson Lyons
NSWC/WOL
Silver Springs, MD 20910

Materials Sciences Corporation
Attn: Dr. B. Rosen
Blue Bell Office Campus
Merion Towle Bldg.
Blue Bell, PA 19422

Materials Sciences Corporation
Attn: Dr. K. Boesking
Blue Bell Office Campus
Merion Towle Bldg
Blue Bell, PA 19422

McDonnell Douglas Astronautics Company
Attn: Mr. L. Greszczuk
5301 Bolsa Avenue
Huntington Beach, CA 92647

McDonnell Douglas Research Laboratories
Attn: H. Holman
PO Box 516
St Louis, MO 63166

Dr. George Meyer
Army Research Office
PO Box 12211
Research Triangle Park, NC 27709

Dr. James S. Murday
Code 208A, Bldg 207
Naval Research Laboratory
Washington, DC 20375

NASA, Marshall Space Flight Center
Attn: Mr. B. Powers, EP 25
Huntsville, AL 35812

Commander
Naval Sea Systems Command
Attn: Mr. M. Kinna (SEA-0352)
Washington, DC 20302

Commander
Naval Surface Weapons Center
Attn: Mr. R. Edwards (Code WA-43)
White Oak Laboratory
Silver Springs, MD 20910